

A new approach to AC microgrids protection using a bi-level multi-agent system

Navid Ghaffarzadeh^{1,*}, Ali Bamshad¹

¹ Faculty of Technical and Engineering, Imam Khomeini International University, Qazvin, Iran

ARTICLE INFO

Article history:

Received 17 January 2022

Received in revised form 28 March 2022

Accepted 04 April 2022

Keywords:

Microgrid protection

Bi-level MAS

Pilot impedance

Symlet DWT

Resilience

Uncertain parameters

DG

ABSTRACT

Nowadays, microgrids are expanding due to their numerous benefits. However, the control and protection of microgrids is a serious challenge. All the implemented plans for the protection of microgrids have drawbacks. This study presents a bi-level multi-agent system (MAS) approach to microgrids protection. The first level is responsible for microgrid lines protection. Firstly, it calculates the pilot impedance of each line. The pilot impedance is a limited number for internal faults of the line, but it is infinite for external faults of the line. so, the line's internal fault is detected by evaluation of pilot impedance with a predetermined value. The second level is responsible for Distributed Generation (DGs) protection. Firstly, it decomposes the DGs output signals by Discrete Wavelet Transform (DWT). Then, it multiplies the summations of the first and second level's details of each signal together as CC index. CC is zero in normal grid conditions and has a negative peak with a sharp negative rate in external faults, and will experience a positive peak with a sharp positive rate for internal faults and changes with a very slow rate in case of grid's natural transitions. So, the agent detects the fault by evaluating the CC. The simulation results in a 5-bus microgrid indicate the proposed scheme protects the microgrid with a reliability of 100% with considering all microgrid's uncertainties.

1. Introduction

A microgrid is defined in different ways from different perspectives. For example, the USA Energy Agency defines a microgrid as: "A microgrid consists of several loads and specific DG sources that can be controlled on their own. The microgrid can also be operated connected to the main grid or separately from it." Or from the perspective of the National Council for Electrical Systems, a microgrid is as: "A microgrid is a distribution network in which there are DG units and types of storage systems and loads, and can be operated separately or connected to the main distribution network [1]."

A concept that is common in all definitions is the presence of DGs in microgrids. In a way, a microgrid integrates DG resources with loads, which has various benefits, including:

- Improves power quality.
- Increases operating efficiency.
- Increases system reliability during power outages.
- Reduces project costs [2].

1.1. Literature review

However, in addition to the benefits of microgrids, and can meet the load's needs without emitting environmental pollution, there have also problems and complexities to control and protection [3]. Traditional distribution systems are often radial and fed from one side. However,

* Corresponding author

E-mail address: ghaffarzadeh@eng.ikiu.ac.ir

<http://dx.doi.org/10.52547/ijrtei.1.1.66>

microgrids contain DG units and can be fed from two sides, either connected to the main grid or separately from the network, which disrupts the protection coordination of the relays [4]. Some researchers proposed overcurrent relays for microgrids protection [5-7]. This approach is simple and economical but further studies should be performed on these plans to separate the short circuit fault from the transient states of the grid and also is influenced by microgrid topology it is more effective in islanded mode [1]. Some authors recommended directional overcurrent relays [8-10]. This approach has an additional complex coordination process and further studies should be performed on these plans to separate the short circuit fault from the transient states of the grid and is more expensive than overcurrent relaying [1].

Some other researchers recommended distance protection [11-13]. The main advantage of this plan is the lack of influence of source impedance. The drawbacks of this plan are the bidirectional power flow, power swing, and high impedance faults can disrupt the protection plan. Also, this plan is influenced by microgrid topology and is expensive [1]. Some other authors recommended implementing the differential protection plans [14,15]. This plan is sensitive and selective, fast and simple, and independent of power swing and fault resistance [1]. Any disturbance in telecommunication links or metering equipment, or delays in telecommunications links, can disrupt the whole plan. This plan is also too expensive [1].

Some researchers also implemented sequence or symmetrical components approaches [16-19]. The most important advantage of using this plan is that the relay settings change during different grid operation conditions and thus, the relay is prepared to detect any further fault [1]. One of the most important weaknesses of this plan is that it requires a lot of telecommunication links, and if any of them is disrupted, the whole plan will be useless. Also, this plan is influenced by microgrid topology and is too expensive [1].

Some other researchers proposed frequency and voltage-based approaches to protect the microgrids [20-23]. One of the important advantages of these plans is that the islanding detection is a low-cost prosecution and it does not have detrimental effect on the power quality. One of the biggest disadvantages of this plan is that there are many unrecognizable zones for the plan [1]. Other researchers proposed some methods based on traveling waves [24,25]. This plan has two main advantages [1]:

- 1) The first advantage is that the location of the fault can be correctly identified.
- 2) The second advantage of this plan is it detects the fault quickly.

Also, this plan has the following drawbacks [1]:

- 1) This plan requires a high sampling rate.
- 2) This plan needs a low-bandwidth communication channel to reach fast action.

Some other researchers proposed the multi-agent system (MAS) approach for protection [26-30]. It is a powerful tool that distributes the task of fault detection across multiple agent systems and in a way, decomposes the protection problem between multiple agent systems. Also, this approach has the following drawbacks [1][31]:

- 1) This plan has a peer-to-peer nature, so the security of the protection plan can be threatened.
- 2) Intelligent agent plan must be done properly to ensure the security and reliability of the plan.
- 3) These schemes often rely on a single CPU, which becomes useless if this CPU is disrupted.
- 4) These plans require telecommunication links, which increases the cost of the plan and the large burden of telecommunication links can disrupt the telecommunication operation, by grid & DG expansion.

1.2. Plan novelty

In this study, a bi-level multi-agent system (MAS) approach has been proposed to protect AC microgrids. the proposed Mas-based approach uses two vigorous techniques that make more powerful agent systems. The first agent detects and clears the faults in microgrid lines by a pilot impedance technique and the second agent detects and clears the internal faults of DGs by a Symlet discrete transform. In this way, the protection burden is decomposed between two agents and each agent has 100% reliability. The main advantages of the proposed plan can summarize as:

- The agents are very fast in fault detection.
- The plan is not dependent on a single CPU because each line has an independent agent.
- The agents need no telecommunication link together. So, the grid or DGs expansion will not influence the plan and there will be no disturbance on the communication link to disrupt the plan operation.
- The plan reliability and selectivity is 100%.
- Due to the lack of telecommunication links usage, which usually costs a lot, the plan will have a reasonable cost.

Various agent system-based schemes have been proposed to protect the distribution networks or microgrids so far. The main superiority of this study over other plans is the plan does not need coordination between protection installations or telecommunication links, while the previously proposed agent systems require coordination between protection installations or use telecommunication links. In some cases, such plans do not perform truly and the plan fails to operate. so the reliability is overshadowed or the cost of the plan increases too much [32-34].

2. Proposed approach

The implemented network in Fig. 4 has two parts. The first part is the network power lines and the second part is the DGs that are connected to the buses. Fig. 1 shows the proposed scheme for the protection of AC microgrid in Fig. 4. Each agent operates independently of the other. The first agent, determines the fault within each line correctly, using the pilot impedance technique. Firstly, the current and voltage samples of each terminal of the line are sent to the agent. It then calculates the impedance for both sides of the line by the pilot impedance equations. Finally, the agent realizes that a fault has occurred by evaluating this impedance.

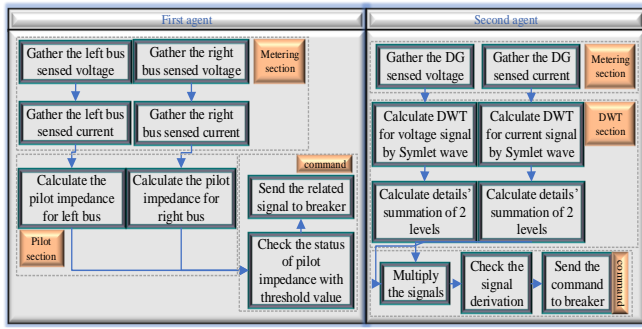


Fig. 1. Proposed agent system schematic

The second agent determines the fault within the DG units using Symlet DWT. First, the second agent receives the current and voltage output samples of each DG's output at its point of common connection (PCC) to the microgrid. It then decomposes the signals using a second level, eight order symlet DWT. Then, the mathematical summation of the first and second-level details of the signal is calculated at each moment. The obtained summations for the voltage signal and the current signal are multiplied by each other, and the agent detects the fault by evaluating the changes' rate of this product.

2.1. First agent

Fig. 2 is part of a microgrid, containing a line between two buses, in which a fault has occurred in this line:

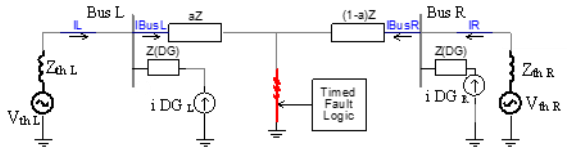


Fig. 2. a line of microgrid with internal fault

A KVL from the left side and right side to the fault point is written according to (1):

$$V_{thL} - V_{thL} \cdot i_L - (\alpha Z)(i_L + i_{DG_L}) = V_{thR} - V_{thR} \cdot i_R - (1 - \alpha)Z(i_R + i_{DG_R}) \quad (1)$$

Where α is the length of faulted line in percent, i_{DG_L} and i_{DG_R} are the left side and right side DG contribution respectively and voltage and current passing through the buses can express as (2) to (5):

$$V_{thL} - V_{thL} \cdot i_L = V_{BusL} \quad (2)$$

$$V_{thR} - V_{thR} \cdot i_R = V_{BusR} \quad (3)$$

$$i_L + i_{DG_L} = i_{BusL} \quad (4)$$

$$i_R + i_{DG_R} = i_{BusR} \quad (5)$$

By interpreting (1) to (5) in (1):

$$V_{BusL} - (\alpha Z)i_{BusL} = V_{BusR} - (1 - \alpha)Zi_{BusR} \quad (6)$$

$$V_{BusL} - V_{BusR} + Zi_{BusR} = (\alpha Z)i_{BusL} + (\alpha Z)i_{BusR} \quad (7)$$

By adding $\left(\frac{Z}{Z_{DG_L}}V_{BusL}\right)$ to both sides of (7):

$$V_{BusL} - V_{BusR} + Zi_{BusR} + \frac{Z}{Z_{DG_L}}V_{BusL} = (\alpha Z)(i_{BusL} + i_{BusR}) + \frac{Z}{Z_{DG_L}}V_{BusL} \quad (8)$$

By dividing both sides of (8) to $(i_{BusL} + i_{BusR})$:

$$\frac{V_{BusL} - V_{BusR} + Zi_{BusR} + \frac{Z}{Z_{DG_L}}V_{BusL}}{i_{BusL} + i_{BusR}} = \alpha Z + \frac{\frac{Z}{Z_{DG_L}}V_{BusL}}{i_{BusL} + i_{BusR}} \quad (9)$$

Where the left side of (9) is considered as the pilot impedance in point aspect of the left bus:

$$Z_{pilotL} = \frac{V_{BusL} - V_{BusR} + Zi_{BusR} + \frac{Z}{Z_{DG_L}}V_{BusL}}{i_{BusL} + i_{BusR}} \quad (10)$$

Also (6) can be rewritten as:

$$V_{BusR} - V_{BusL} = Zi_{BusR} - (\alpha Z)i_{BusR} - (\alpha Z)i_{BusL} \quad (11)$$

By adding $\left(Zi_{BusL} + \frac{Z}{Z_{DG_R}}V_{BusR}\right)$ to both sides of (11):

$$V_{BusR} - V_{BusL} + Zi_{BusL} + \frac{Z}{Z_{DG_R}}V_{BusR} = (Z)(i_{BusL} + i_{BusR}) - (\alpha Z)(i_{BusL} + i_{BusR}) - \frac{Z}{Z_{DG_R}}V_{BusR} \quad (12)$$

By dividing both sides of (12) to $(i_{BusL} + i_{BusR})$:

$$\frac{V_{BusR} - V_{BusL} + Zi_{BusL} + \frac{Z}{Z_{DG_R}}V_{BusR}}{i_{BusL} + i_{BusR}} = (1 - \alpha)Z + \frac{\frac{Z}{Z_{DG_R}}V_{BusR}}{i_{BusL} + i_{BusR}} \quad (13)$$

Where the left side of (13) is considered as the pilot impedance in point aspect of the right bus:

$$Z_{pilotR} = \frac{V_{BusR} - V_{BusL} + Zi_{BusL} + \frac{Z}{Z_{DG_R}}V_{BusR}}{i_{BusL} + i_{BusR}} \quad (14)$$

But for an external fault as depicted in Fig. 3:

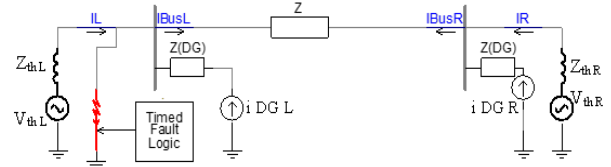


Fig. 3. a line of microgrid with external fault

(15) & (16) can be expressed as:

$$i_{BusL} = \frac{V_{BusL} - V_{BusR}}{Z} \quad (15)$$

$$i_{BusR} = \frac{V_{BusR} - V_{BusL}}{Z} \quad (16)$$

By implementation of (15) & (16) in pilot impedance of right bus and left bus, (17) is concluded for external faults:

$$Z_{pilotR} = Z_{pilotL} = \infty \quad (17)$$

Therefore, if the calculated pilot impedance is larger than the threshold value, it means that a fault has occurred outside the line and there is no need to operation of breakers of line, but if the output impedance has less than the threshold, This means that the fault occurred inside the protected line and the breakers at both ends of the line must operate and isolate the line. This is because a microgrid can be non-radial as shown in Fig. 4 and if the line is broken on one side, the fault is still fed on the other side. The threshold value of agent operation is also set at 3000.

This threshold has been set to distinguish some possible transient states, such as sudden changes in load, and output power of renewable units, with faults. Each change in load and renewables output is expressed with its normal probability function in this study.

2.2. Second agent

Initially, the current and voltage signals of each solar and wind unit, are sampled and sent to the second agent right at the PCC of units to the microgrid. Then each signal is decomposed as:

$$\text{DG output current signal: } \rightarrow (g^1, h^1) \quad (18)$$

$$\text{DG output voltage signal: } \rightarrow (g^1, h^1) \quad (19)$$

Where:

$$g^1 \text{ current signal: } \rightarrow (g^2, h^2) \quad (20)$$

$$g^1 \text{ voltage signal: } \rightarrow (g^2, h^2) \quad (21)$$

So:

$$\text{current signal: } \rightarrow (g^2, h^2, h^1) \quad (22)$$

$$\text{voltage signal: } \rightarrow (g^2, h^2, h^1) \quad (23)$$

where:

$$g^n = (g_1^n, g_2^n, g_3^n, g_4^n, g_5^n, g_6^n, g_7^n, g_8^n) \quad (24)$$

$$h^n = (h_1^n, h_2^n, h_3^n, h_4^n, h_5^n, h_6^n, h_7^n, h_8^n) \quad (25)$$

The current signal of each DG can be decomposed as (26):

$$\text{current DWT} = \sum_{k=1}^N h^1 I_{-DG}(k) + \sum_{k=1}^N h^2 I_{-DG}(k) \quad (26)$$

The voltage signal of each DG can be decomposed as (27):

$$\text{voltage DWT} = \sum_{k=1}^N h^1 V_{-DG}(k) + \sum_{k=1}^N h^2 V_{-DG}(k) \quad (27)$$

Where the N is the order of DWT that has been set on 8. Then the CC index is defined according to (28):

$$\text{CC index} = \text{current DWT} \times \text{voltage DWT} \quad (28)$$

Then the agent system calculates the rate of changes of the CC index. Two scenarios May happen:

A) If $\frac{d(CC)}{dt} > 0$, the fault is inside of DG.

B) If $\frac{d(CC)}{dt} < 0$, the fault is outside of DG.

This index will experience a sharp negative rate if the fault occurred outside of the DG unit. If this fault has occurred within the DG unit, this index will experience a sharp positive change. So, the derivation of the CC index is sent to the second agent's relay. The threshold margin value of this agent is considered to be 1300.

3. Results and discussion

In this section, the implemented network case study is interpreted at first, and then the proposed plan is implemented on the under-study network.

3.1. Implemented case study

To implement the proposed plan, a 5-bus microgrid is implemented according to Fig. 4:

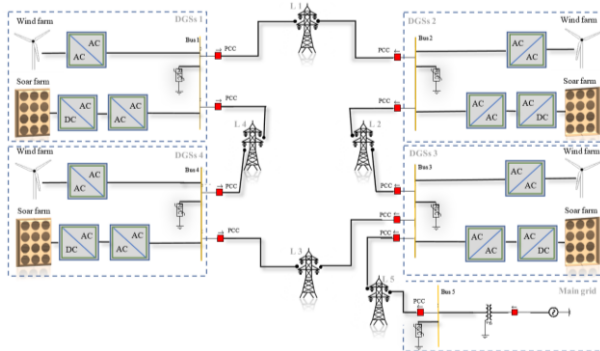


Fig. 4. understudy microgrid

circular grids have the following advantages over radial grids:

- 1) They have less blackout compared to the radial grid.
- 2) They don't need to use maneuver lines.
- 3) There is no worry about the insulation failure of the lines.

Also, the technical characteristics of photovoltaic panels can be expressed by Table. 1:

Solar panels characteristics	
Peak power (WP)	335
Open circuit voltage (V)	46.24
Short circuit current (A)	9.30
Voltage at Pmax (V)	38.12
Current at Pmax (A)	8.79
Efficiency (%)	17.19
Dimension (mm)	992*1964*35
Weight (Kg)	21.6 (+/-0.1)
Irradiation rate limit (in PSCAD)	1000 [1/s] / (W/m ² /sec)
Temperature rate limit (in PSCAD)	5 [1/s] / (C/sec)
Fire safety classification	Class C
Number of series modules per array	36
Number of parallel modules per array	24
Number of cells per panel	72

And the tie-line characteristics are depicted according to Table. 2:

Tie line	R(ohm)	L (mH)
L ₁	0.38 Ω	0.23 mH
L ₂	0.45 Ω	0.16 mH
L ₃	0.49 Ω	0.29 mH
L ₄	0.71 Ω	0.32 mH
L ₅	0.65 Ω	0.18 mH

Also, the technical characteristics of wind units are represented by Table. 3:

windfarm characteristics	
Rated power	2000kW
Cut-in wind speed	4m/s
Rated wind speed	13m/s
Cut-out wind speed	25m/s
Rotor diameter	90 m
Number of blades	3
Max rotor speed	14.9 U/min
Gearbox efficiency	97%
Governor proportional gain	6.2 [deg/p.u]
Governor integral gain	6.2
Governor deferential gain	0.05 [deg/p.u]
Governor gain multiplier	30 [deg/pu]
Tip speed	70 m/s
tower height	80*95*105 m

The following uncertainties are also considered for the network:

- 1) load uncertainty
- 2) Connection or disconnection from the main grid
- 3) Type of fault
- 4) fault impedance
- 5) fault location
- 6) Output of wind and solar units

These uncertainties are implemented according to the Table. 4:

parameter	Different status
Wind capacity	Wind speed=Norm (13,4)
PV capacity	Temp= Norm (40-10), Irrad= Norm (1200-200)
Fault location	Lines (#1-2-3-4-5), DGs (#6- 7-8-9)
Fault type	1 ϕ (AG)- 2 ϕ (ABG)- 3 ϕ (ABCG)
Fault impedance	Bolt-10 Ω -30 Ω -60 Ω
Connection to main grid load	Connect (1), disconnect (0) Norm (70,20Kw – 40,15Kvar)

Fault locations of #6-7-8-9 refer to fault inside of in DGs 1,2,3,4 respectively and fault location of #1-2-3-4-5 refers to a fault in lines of 1,2,3,4,5 respectively.

Uncertainties in the form of lists, such as fault location, fault type, fault impedance, and grid operation mode, do not require sampling and are defined as numbers (real or binary) for the Multiplerun module. Uncertainties, which are in the form of probability density function (PDF), are sampled using the CDF⁻¹ method in Excel software in the first step. Then, the samples are entered into the Multiplerun module as the real numbers. Finally, all the uncertainties are implemented simultaneously in the Multiplerun block during simulation.

3.2. Simulation results

Uncertainties considered as normal PDFs, always change throughout the simulation independently. Other parameters such as fault location, fault impedance, type of fault, connection or disconnection of the microgrid from the main grid also created a total of 216 different states. Also, ten samplings were performed for PDFs using the library Monte Carlo method in each different 216 states. This means that ten sets of sampling are performed for each of these 216 cases. Eventually, 2160 different modes emerge. Table. 5 depicts the implemented agent's operation on line 3, under all 2160 different modes:

Table. 5a. L3 agent operation for fault in its zone

	First agent relay command on L3	second agent relay command on DGs
uncertainty		
$R_{load} \sim N(70,$ 20Kw 40,15Kvar)		
Wind speed $\sim N$ (13, 4)		
temp $\sim N$ (40, 10)		
Irrad $\sim N$ (1200,200)		
Fault type (1-2-3 phase)	1	0
Fault impedance (0-10-30-60)		
Fault location (#3)		
PCC (0-1)		

Table. 5b. L3 agent operation for external faults 1 to 5

	First agent relay command on L3	second agent relay command on DGs
uncertainty		
$R_{load} \sim N(70,$ 20Kw 40,15Kvar)		
Wind speed $\sim N$ (13, 4)		
temp $\sim N$ (40, 10)		
Irrad $\sim N$ (1200,200)		
Fault type (1-2-3 phase)	0	0
Fault impedance (0-10-30-60)		
Fault location (#1-2-4-5)		
PCC (0-1)		

Table. 5c. L3 agent operation for external faults 6 to 9

uncertainty	First agent relay command on L3	second agent relay command on DGs
$R_{load} \sim N(70, 20Kw 40,15Kvar)$		
Wind speed $\sim N(13, 4)$		
temp $\sim N(40, 10)$		
Irrad $\sim N(1200,200)$		
Fault type (1-2-3 phase)	0	1
Fault impedance (0-10-30-60)		
Fault location (#6-7-8-9)		
PCC (0-1)		

Table. 6b. DG 4 agent action for external faults 6 to 8

uncertainty	First agent relay command on lines	second agent relay command on DGs' 4
$R_{load} \sim N(70, 20Kw 40,15Kvar)$		
Wind speed $\sim N(13, 4)$		
temp $\sim N(40, 10)$		
Irrad $\sim N(1200,200)$		
Fault type (1-2-3 phase)	0	0
Fault impedance (0-10-30-60)		
Fault location (#6-7-8)		
PCC (0-1)		

Table. 6 depicts the implemented agent's operation on the DG 4, under all 2160 different modes. A fault has occurred in the wind generator.

Table. 6a. DG 4 agent action for external faults 1 to 5

uncertainty	First agent relay command on lines	second agent relay command on DGs' 4
$R_{load} \sim N(70, 20Kw 40,15Kvar)$		
Wind speed $\sim N(13, 4)$		
temp $\sim N(40, 10)$		
Irrad $\sim N(1200,200)$		
Fault type (1-2-3 phase)	0	0
Fault impedance (0-10-30-60)		
Fault location (#1-2-3-4-5)		
PCC (0-1)		

Table. 6c. DG 4 agent action for internal fault

uncertainty	First agent relay command on lines	second agent relay command on DGs' 4
$R_{load} \sim N(70, 20Kw 40,15Kvar)$		
Wind speed $\sim N(13, 4)$		
temp $\sim N(40, 10)$		
Irrad $\sim N(1200,200)$		
Fault type (1-2-3 phase)	0	1
Fault impedance (0-10-30-60)		
Fault location (#9)		
PCC (0-1)		

Also, Fig. 5 depicts the operation of 2 agents under different fault locations:

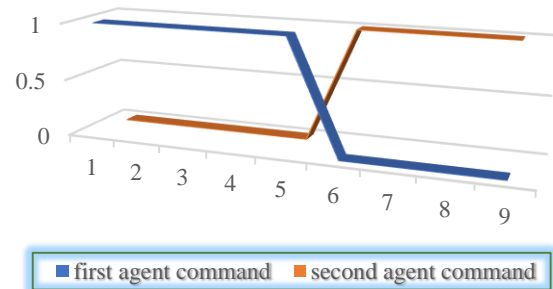


Fig. 5. agent's operation in different locations

Fig. 5 demonstrates the first agent system operates for faults in zones 1 to 5 where is its protection zone, and the relay output is equal to 1. On the other hand, the agent output is zero for faults in zones 6 to 9 where is not its zone and the agent does not act truly.

Also, the second agent system operates for faults in zones 6 to 9 where is its protection zone, and the relay output is equal to 1. On the other hand, the agent output is zero for faults in zones 1 to 5 where is not its zone and the agent does not act truly. This means the reliability and selectivity of the agents are 100%.

Figs. 6 & 7 depicts the first agent decision signal for the internal and external faults in line 1 for grid disconnected mode:

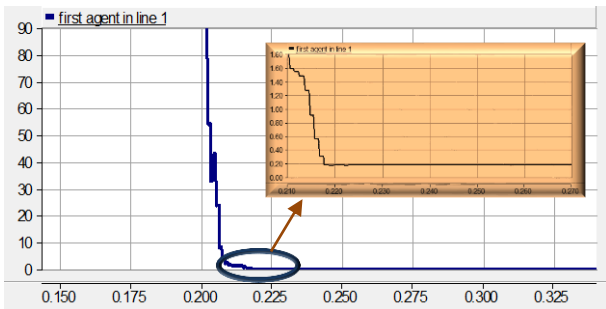


Fig. 6. 1st agent decision signal (2ϕ , 30Ω fault in L1)

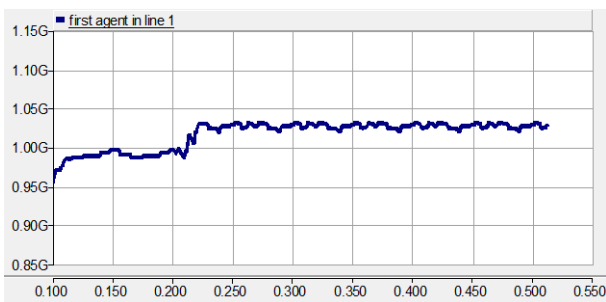


Fig. 7. 1st agent decision signal (2ϕ , 30Ω fault out of L1)

as it is visible in Figs 6 and 7, the almost constant and finite value of pilot impedance is related to an internal fault but a huge value for pilot impedance is related to an external fault for a line.

Also, Figs 8 to 11 depict the voltage and current waveforms for the internal 3 phase, bolt fault in 40% of the initial line 1 near to bus 1 in grid-connected mode:

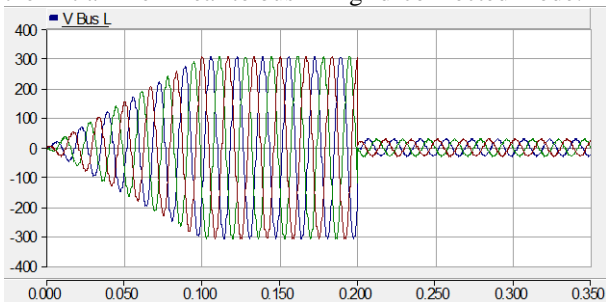


Fig. 8. voltage waveform in aspect of bus 1 (L1 fault)

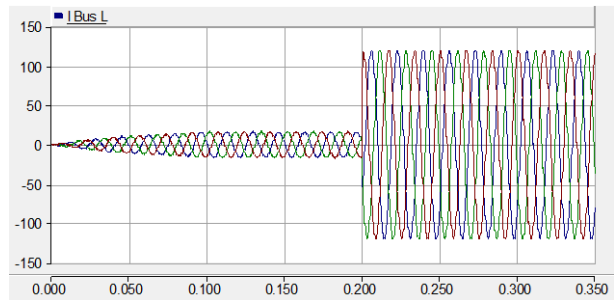


Fig. 9. current waveform in aspect of bus 1 (L1 fault)

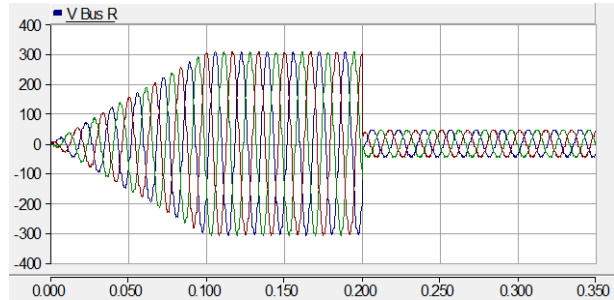


Fig. 10. voltage waveform in aspect of bus 2 (L1 fault)

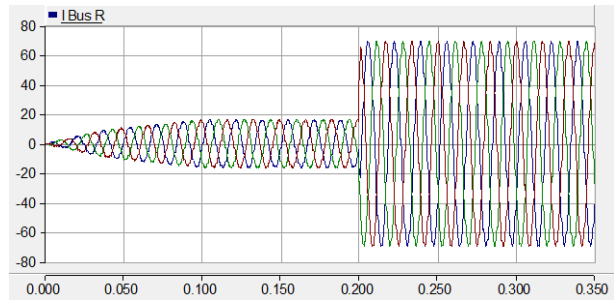


Fig. 11. current waveform in aspect of bus 2 (L1 fault)

Figs. 12 and 13 depict the second agent decision signal for the internal and external faults in DG 2 for grid disconnected mode:

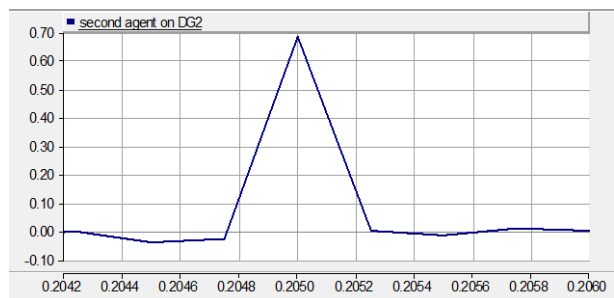


Fig. 12. 2nd agent decision signal (3ϕ , 30Ω fault in PV unit of DG2)

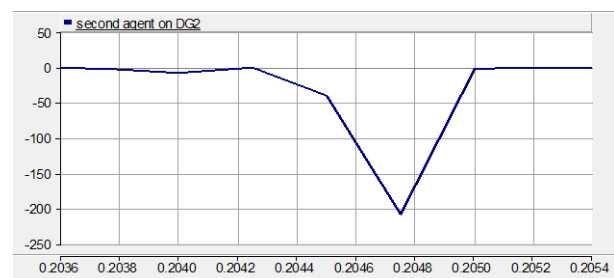


Fig. 13. 2nd agent decision signal (3ϕ , 30Ω fault in L2)

as it is visible in Figs 12 & 13, the incremental ramp rate in the input signal of the second agent system meaning to an internal fault, and incremental ramp rate meaning to an external fault.

4. Conclusion

The presence of distributed generation sources in a microgrid changes its radial nature. This can cause conventional protection schemes to maloperation or be disrupted completely. Various approaches have been proposed to resolve this problem by researchers. But each plan has its drawbacks including the plan's cost, the poor performance of the plan in some conditions that threaten the reliability, complex online calculations, etc. In this study, a bi-level multi-agent system is presented for AC microgrid protection. The first level detects any faults on lines in less than one cycle using the pilot impedance technique and sends the trip command to the breaker. The second agent detects any faults within the distributed generations using a Discrete Wavelet Transform in maximum of 5 milliseconds and sends the trip command to the breaker. Therefore, the operational advantages of the plan can be summarized as:

- 1) High-performance speed in fault detection
- 2) Requires current and voltage samples only
- 3) Any disruption in an agent operation does not influence other agents and doesn't disrupt the other agents.

Also, the proposed plan has a reasonable cost to implement and has 100% reliability.

5. References

- [1] B. Patnaik, M. Mishra, R. C. Bansal, and R. K. Jena, "AC microgrid protection – A review: Current and future prospective," *Appl. Energy*, vol. 271, no. May, pp. 115-210, 2020.
- [2] A. Bamshad, O. Safarzadeh, "Effects of the move towards Gen IV reactors in capacity expansion planning by total generation cost and environmental impact optimization." *Nucl. Eng. Technol.*, vol. 53, no. April, pp.1369–1377, 2021.
- [3] P. T. Manditereza, R. C. Bansal, "Review of technical issues influencing the decoupling of DG converter design from the distribution system protection strategy," *IET Renew. Power Gener.*, vol. 12, no. 10, pp. 1091–1100, 2018.
- [4] D.A. Gadanayak, "Protection algorithms of microgrids with inverter interfaced distributed generation units—A review" *Electric Power Systems Research*, vol. 192, no. march, pp.106986, 2021.
- [5] A.E.C. Momesso et al, "Adaptive directional overcurrent protection considering stability constraint," *Electric Power Systems Research*, vol. 181, no. 106190, pp. 0378-7796, 2020.
- [6] M. Irfan, A. Wadood, T. Khurshaid, et al; "An Optimized Adaptive Protection Scheme for Numerical and Directional Overcurrent Relay Coordination Using Harris Hawk Optimization". *Energies*, vol. 14, no. 18, pp. 1996-1073, 2021.
- [7] A. E. C. Momesso, W. Maycon, S. Bernardes, E. N. Asada, "Electrical Power and Energy Systems Fuzzy adaptive setting for time-current-voltage based overcurrent relays in distribution systems," *Electr. Power Energy Syst.*, vol. 108, no. August 2018, pp. 135–144, 2019.
- [8] M.A. Elsadd, T.A. Kawady, A.M.I. Taalab, et al, "Adaptive optimum coordination of overcurrent relays for deregulated distribution system considering parallel feeders." *Electr Eng.*, vol. 103, no. January 2021, pp. 1849–1867, 2021.
- [9] J.A. O. Wilches; A.J. U. Farfan; E.A. Cano-Plata, "Modeling of a Communications-based Directional Overcurrent Protection Scheme for Microgrids," 2018 IEEE ANDESCON confrence, 22-24 Aug. 2018.
- [10] M.H. Sadeghi, et al, "Optimal coordination of directional overcurrent relays in distribution systems with DGs and FCLs considering voltage sag energy index" *Electric Power Systems Research*, vol. 191, no. 106884, pp. 0378-7796, 2021.
- [11] A. M. Tsimitsios, G. N. Korres, V. C. Nikolaidis, "A pilot-based distance protection scheme for meshed distribution systems with distributed generation," *Int. J. Electr. Power Energy Syst.*, vol. 105, no. 8, pp. 454–469, 2019.
- [12] Y. Yin, Y. Fu, Z. Zhang and A. Zamani, "Protection of Microgrid Interconnection Lines Using Distance Relay With Residual Voltage Compensations," in *IEEE Transactions on Power Delivery*, vol. 37, no. 1, pp. 486-495, Feb. 2022.
- [13] B. K. Chaitanya, A. Yadav, and M. Pazoki, "An improved differential protection scheme for micro-grid using time-frequency transform," *Electr. Power Energy Syst.*, vol. 111, no. September 2018, pp. 132–143, 2019.
- [14] T. S. Aghdam, H. K. Karegar, H. H. Zeineldin, "Variable Tripping Time Differential Protection for Microgrids Considering DG Stability," *IEEE Trans. smart grid*, vol. 3053, no. c, pp. 2407 – 2415, 2018.
- [15] V. C. Nikolaidis, G. Michaloudis, A. M. Tsimitsios, D. Tzelepis, C. D. Booth, "A Coordinated Multi-Element Current Differential Protection Scheme for Active Distribution Systems," *IEEE Transactions on Power Delivery*, vol. {}, no. {}, pp. {}, February 2022.
- [16] Ansari, Salauddin, Gupta, O. Hari, "Differential positive sequence power angle-based microgrid feeder protection" *International Journal of Emerging Electric Power Systems*, vol. 22, no. 5, pp. 525-531, 2021.
- [17] D. Library, "Sequence currents based adaptive protection approach for DNs with distributed energy resources," *IET Gener. Transm. Distrib.*, Vol. 11, no. 1, pp. 154–165, 2017.
- [18] N. K. Sharma, S. R. Samantaray, "PMU Assisted Integrated Impedance Angle-Based Microgrid Protection Scheme," *IEEE Transactions on Power Delivery*, vol. 35, no. 1, pp. 183-193, Feb. 2020.
- [19] B. Wang, L. Jing, "A Protection Method for Inverter-based Microgrid Using Current-only Polarity Comparison," *Journal of Modern Power Systems and Clean Energy*, vol. 8, no. 3, pp. 446-453, May 2020.
- [20] M. J. Daryani, A. E. Karkevandi, O. Usta, "Harmonics Content and Voltage Signal Based Hybrid Backup Scheme for Protection of Microgrid Under Different Contingencies," 2019 IEEE PES Innovative Smart Grid Technologies Europe (ISGT-Europe) confrence, pp. 1-5, 2019.
- [21] R. R. Xwkdvdn, "Modeling of rate of change of under frequency relay for microgrid protection," 5 th Int. Electr. Eng. Congr. pattaya, pp. 6–9, 2017.
- [22] M.A.U. Khan, Q. Hong, A. Dyško, C. Booth, "An Active Protection Scheme for Islanded Microgrids", 15th International Conference on Developments in Power System Protection (DPSP 2020), 9-12 March 2020.
- [23] S. Ranjbar, A.R. Farsa, S. Jamali "Voltage - based protection of microgrids using decision tree algorithms," *Int Trans Electri Energy Syst*, vol. 30, no. November, pp. 1 – 15, April 2020.
- [24] M. Asim, S. M. S. Hussain, I. Ali, T. Selim, "Electrical Power and Energy Systems Dynamic protection of power systems with high penetration of renewables : A review of the traveling wave based fault location techniques," *Electr. Power Energy Syst*, vol. 114, no. July 2019, pp. 0142-0615, 2020.
- [25] R. Montoya, B.P. Poudel, A. Bidram, M.J. Reno, "DC microgrid fault detection using multiresolution analysis of traveling waves" *Electr. Power Energy Syst*, vol. 135, no. Febreary 2022, pp. 0142-0615, 2022.
- [26] I. M. Faria, R. H. Furlan, P. E. T. Martins, T. S. Menezes, M. Oleskovicz, D. V. Coury, "The Proposition of a Multiagent System for Adaptive Protection of a Distribution System," 2018 Simposio Brasileiro de Sistemas Eletricos (SBSE) confrence, pp. 1–6, 12-16 May 2018.
- [27] Y. Zheng, Y. Song, D. J. Hill, Y. Zhang, "Multi-Agent System Based Microgrid Energy Management via Asynchronous Consensus ADMM," *IEEE Trans. Energy Convers.*, vol. 8969, no. c, pp. 1–3, 2018.
- [28] A. Hussain, M. Aslam, S. Muhammad, "N-version programming-based protection scheme for microgrids : A multi-agent system based approach," *Sustain. Energy, Grids Networks*, vol. 6, no. June 2016, pp. 35–45, 2016.
- [29] H. F. Habib, O. Mohammed, "Decentralized Multi-Agent System for Protection and the Power Restoration Process in Microgrids," Ninth Annu. IEEE Green Technol. Conf. Decentralized, pp. 359–365, 2017.
- [30] S. Rahman et al, "Crop Field Boundary Delineation using Historical Crop Rotation Pattern," 8th Int. Conf. Agro-Geoinformatics, pp. 1–5, 2019.
- [31] B. Fani et al, " A fault-clearing algorithm supporting the MAS-based protection schemes," *Int J Electr Power Energy Syst*, vol 103, no. June 2018, pp. 0142-0615, 2018.

- [32] B. Fani, H. Bisheh, A. K. Horestani, "An offline penetration-free protection scheme for PV-dominated distribution systems," *Electr Power Syst Res*, vol. 157, no. April 2018, pp. 1-9, 2018.
- [33] E. Abbaspour, B. Fani, E. H. Forushani, "A bi-level multi agent based protection scheme for distribution networks with distributed generation," *Int J Electr Power Energy Syst*, vol. 112, no. 11, pp. 209-220, 2019.
- [34] B. Fani, M. Dadkhah, A. K. Horestani, "Adaptive protection coordination scheme against the staircase fault current waveforms in PV-dominated distribution systems." *IET Gener. Transm. Distrib*, Vol. 12 no. 9, pp. 2065-2071, 2018.